jove

Dual Raster-Scanning Photoacoustic Small-Animal Imager for Vascular Visualization

Fei Yang[1,2], **Zhiyang Wang**[1,2], **Sihua Yang**[1,2]

[1] MOE Key Laboratory of Laser Life Science & Institute of Laser Life Science, College of Biophotonics, South China Normal University [2] Guangzhou Provincial Key Laboratory of Laser Life Science, College of Biophotonics, South China Normal University

Corresponding Author

Sihua Yang
yangsh@scnu.edu.cn

Citation

Yang, F., Wang, Z., Yang, S. Dual Raster-Scanning Photoacoustic Small-Animal Imager for Vascular Visualization. *J. Vis. Exp.* (161), e61584, doi:10.3791/61584 (2020).

Date Published

July 15, 2020

DOI

10.3791/61584

URL

jove.com/video/61584

Abstract

Imaging of vascular networks on small animals has played an important role in basic biomedical research. Photoacoustic imaging technology has great potential for application in the imageology of small animals. The wide-field photoacoustic imaging of small animals can provide images with high spatiotemporal resolution, deep penetration, and multiple contrasts. Also, the real-time photoacoustic imaging system is desirable to observe the hemodynamic activities of small-animal vasculature, which can be used to research the dynamic monitoring of small-animal physiological features. Here, a dual-raster-scanning photoacoustic imager is presented, featuring a switchable double-mode imaging function. The wide-field imaging is driven by a two-dimensional motorized translation stage, while the real-time imaging is realized with galvanometers. By setting different parameters and imaging modes, in vivo visualization of small-animal vascular network can be performed. The real-time imaging can be used to observe pulse change and blood flow change of drug-induced, etc. The wide-field imaging can be used to track the growth change of tumor vasculature. These are easy to be adopted in various areas of basic biomedicine research.

Introduction

In the basic biomedical field, small animals can simulate human physiological function. Therefore, small-animal imaging plays an important role in guiding the research of human homologous diseases and seeking effective treatment[1]. Photoacoustic imaging (PAI) is a non-invasive imaging technique combining the advantages of optical imaging and ultrasound imaging[2]. Photoacoustic microscopy (PAM) is a valuable imaging method for basic research of small animal[3]. PAM can easily obtain high-resolution, deep-penetration, high-specificity and high-contrast images based on optical excitation and ultrasound detection[4].

A pulse laser with a specific wavelength is absorbed by endogenous chromophores of tissues. Subsequently, the temperature of the tissue rises, which results in the production

of photo-induced ultrasonic waves. The ultrasonic waves can be detected by an ultrasonic transducer. After signal acquisition and image reconstruction, the spatial distribution of the absorber can be obtained[5]. On the one hand, the visualization of whole-organ vascular network requires a wide field of view. The process of wide-field scanning usually takes a long time to ensure high-resolution[6,7,8]. On the other hand, observing the hemodynamic activities of small animals requires fast real-time imaging. The real-time imaging is beneficial to study the vital signs of small animals in real time[9,10,11]. The field of view of real-time imaging is usually sufficiently small to ensure a high update rate. Thus, there is often a tradeoff between achieving a wide field of view and real-time imaging. Previously, two different systems were used for wide-field imaging or real-time imaging, separately.

This work reports a dual raster-scanning photoacoustic imager (DRS-PAI), which integrated wide-field imaging based on a two-dimensional motorized translation stage and real-time imaging based on a two-axis galvanometer scanner. The wide-field imaging mode (WIM) is performed to show vascular morphology. For the real-time imaging mode (RIM), there are currently two functions. First, RIM can provide real-time B-scan images. By measuring the displacement of vasculature along the depth direction, the characteristics of respiration or pulse can be revealed. Second, the RIM can quantitatively measure the specific area in the WIM image. By providing comparable images of local WIM regions, the details of the local change can be accurately revealed. The system designs a flexible transition between wide-field imaging of vascular visualization and real-time imaging of the local dynamic. The system is desirable in basic biomedical research where there is a need for small-animal imaging.

Protocol

All animal experiments were performed in compliance with guidelines provided by the institutional animal care and use committee of South China Normal University, Guangzhou, China.

1. System Setup

1. Optical path (**Figure 1**)
    1. Use a 532 nm pulse laser as the system laser source. Set the repetition rate of the laser to 10 kHz, the output energy to 100% and the trigger setting to external trigger using a user-defined program.
    2. Couple the laser beam to single-mode fiber (SMF) via an optical fiber coupler (FC1). Collimate the laser beam using an optical fiber collimator (FC2) on a two-dimensional motorized stage (Motor, maximum speed: 20 mm/s).
    3. Deflect the laser beam using a two-axis galvanometer scanner (Galva). Use a moveable mirror (M1) to reflect the beam. Focus the beam through a 4× objective lens (OL, Numerical aperture: 0.1).
    4. Use an XY translator mount (TM) to fix the self-made hollow ultrasonic transducer (UT, Central frequency: 25 MHz; Bandwidth: more than 90%; Center hole: 3 mm) on the bottom of the OL[12]. Pass the focused beam through the center hole of the ultrasonic transducer.
2. Scanning path
    1. Lock the Galva using a field-programmable gate array (FPGA 2) during WIM. Set the appropriate

scanning range and scanning speed by a user-defined program.

2. Lock the Motor using a field-programmable gate array (FPGA 1) during RIM. Set the scanning frequency and number of scanning points using FPGA 2. Use a user-defined program to control the start and stop scanning.

3. Data acquisition

1. Use a 50-dB amplifier (AMP) to amplify the PA signal. Digitize the signal by the data acquisition card (DAQ). Obtain the trigger signal through FPGA 1 or FPGA 2.

2. Use a graphics processing unit (GPU) to process data and display images in parallel[13].

4. CCD imaging system

1. Use a ring-shaped white LED (Color temperature: 6500 K; Illuminance: 40000 lux; Diameter: 7.5 cm) as a lighting source. Remove M1, use a fixed mirror (M2) to reflect the light.

2. Record the images using a CCD camera (6.3 million pixels) on the PA imaging system. Display the images with a display software.

2. System alignment

1. Select a water tank (10 cm × 10 cm × 4.4 cm; bottom window: 3 cm × 3 cm). Cover the entire water tank using a polyethylene membrane (membrane thick: 10 μm). Add sufficient ultrapure water.

2. Place the water tank on the working stage.

3. Turn on the laser switch. Select the laser control program. Preheat for 5 min. Press the “ON” button on the pumping switch. Set the laser parameters as per step 1.1.1. Open the baffle of the laser.

4. Select the A-line collected program. Press the “Start” button to capture the single point signal and display amplitude and spectrum of the current A-line signal.

5. Place a blade at the bottom of the water tank. Immerse the bottom part of UT in the water tank for acoustic coupling. Avoid bubbles in the bottom part of UT.

6. Adjust the position of Galva, adjust XY translator between UT and OL to avoid oscillation signal, and make sure this is confocal.

7. Adjust the height of the working stage to maximize the amplitude of the signal, and determine the focus position.

3. Animal experiment

1. Use a 5–6 weeks old BALB/c mouse with a bodyweight of 20–30 g.

2. Anesthetize the animal using urethane (1 g/kg) injected intraperitoneally before the experiment.

3. Conduct transition between WIM and RIM.

1. Use a planar ultrasonic transducer. Shave the fur on the back of the mouse using a trimmer and depilatory cream. Place the mouse on the holder (8 cm × 2.8 cm × 2 cm) in prone position.

2. Allow the imaging region to be in contact with the polyethylene membrane using ultrasound gel. Avoid bubbles in the contact part.

3. Place the holder on the working stage for acoustic coupling. Follow steps 2.3–2.4 to start the laser and collect A-line signal. Follow steps 2.6–2.7 to align. Press “Stop” to end the collection after alignment.

4. Select the WIM program. Name the newly created folder. Set the scanning parameter at to 20 mm/s in the “Scanning Speed” tab, “20 mm*20 mm” in the

"Scanning Area" tab, and "20" in the "Step" tab. Click the **Collect** button to start scanning.

5. Click the **Stop** button to end scanning after acquisition. Click **Return to Zero** to bring the Motor to zero. Close the laser baffle. Set the trigger setting to internal trigger. Press the **OFF** button for pumping switch.
6. Replace WIM trigger as RIM trigger and connect it to the external laser trigger. Press the **ON** button for pumping switch. Set the trigger setting to the external trigger. Click the **Exit** button to exit the WIM program.
7. Use step 2.4 to collect the A-line signal. Open the laser baffle. Follow steps 2.6–2.7 to align. Press **Stop** to end collection after alignment.
8. Select the RIM program. Name the newly created folder. Click the **Collect** button to start scanning.
9. Click the **Stop** button to end scanning after completing acquisition. Click the **Exit** button to exit the RIM program.

4. Conduct WIM of vascular visualization.
    1. Use a focused ultrasonic transducer (Central frequency: 25 MHz; Bandwidth: more than 90%; Focal length: 8 mm). Remove the hair of mice ear or scalp.
        1. Use a scalpel to make a small incision on the lateral side of the cranial temporal top of the mouse (depth to the skull). Use ophthalmic scissors to start from this incision. Cut the scalp around the outer side of the skull. Compress the bleeding point to stop bleeding. Wash the wound with normal saline. Place the mouse on the holder.
    2. Allow the imaging region to be in contact with the polyethylene membrane using ultrasound gel. Avoid bubbles in the contact region (**Supplementary Figure 1**).
    3. Place the holder on the work stage for acoustic coupling. Use steps 2.3–2.4 to open laser and collect A-line signal. Use step 2.6–2.7 to align. Press **Stop** to end collection after alignment.
    4. Select WIM program. Name the newly created folder. Set the scanning parameter to "10 mm/s" in the "Scanning Speed" tab, "10 mm*10 mm" under the "Scanning Area" tab, and "10" in the "Step" tab. Click the **Collect** button to start scanning.
    5. Click the **Stop** button to end scanning after completing acquisition. Click the **Return to Zero** to make the Motor return to zero. Click the **Exit** button to exit the WIM program.
5. Conduct RIM for dynamic monitoring of small animals.
    1. Shave the hair of the mouse abdomen. Place the mouse on the holder in supine position.
    2. Allow the imaging region to be in contact with the polyethylene membrane using ultrasound gel. Avoid bubbles in the contact region.
    3. Place the holder on the work stage for acoustic coupling. Perform steps 2.3–2.4 to start the laser and collect A-line signal. Perform step 2.6–2.7 to align. Press **Stop** to end collection after alignment.
    4. Select the RIM program. Name the newly created folder. Click the **Collect** button to start scanning.
    5. Click the **Stop** button to end scanning after completing acquisition. Click the **Exit** button to exit the RIM program.

6. Use the RIM data for reconstruction of the maximum amplitude projection (MAP) along the depth direction by user-defined program. Observe the dynamic changes in the animal.

Representative Results

The schematic of the DRS-PAI is shown in **Figure 1**. The system allows flexible and repeatable switching between WIM with RIM. The acquired PA signal is processed quickly to generate PA B-Scan and MAP images. The CCD camera can provide photographs of samples.

All components of the DRS-PAI are integrated and assembled in an imager setup (**Figure 2**), making it easy to assemble and operate. In the WIM, continuous raster scanning of a two-dimensional motorized stage is used. The signal of the running stage is recorded. The data acquisition proceeded during uniform translation of the stage. In the RIM, a two-axis galvanometer scanner was used. The data were collected synchronously with the Galva scanning (**Figure 3**).

Here, the vascular images of samples with each imaging mode were collected. **Figure 4A** shows the MAP image of the mouse back in WIM. The imaging time was about 33 min. **Figure 4B** shows B-scan images of mouse back during RIM. The whole process of RIM is shown in **Video 1**. Then, a focused ultrasonic transducer was used. The vascular networks of the mouse ear and brain are shown in **Figure 5**. The imaging time was about 16 min. This demonstrates the ability of DRS-PAI to image wide-field vasculature. In addition, **Figure 6A** shows that the imaging range contains a vessel. The imaging range of RIM is about 100 μm due to the use of the focused ultrasonic transducer. The displacement image along the depth direction of the mouse abdomen versus time is shown in **Figure 6B**. **Video 2** shows the process of vascular displacement and obtaining the current pulse or respiration curve.

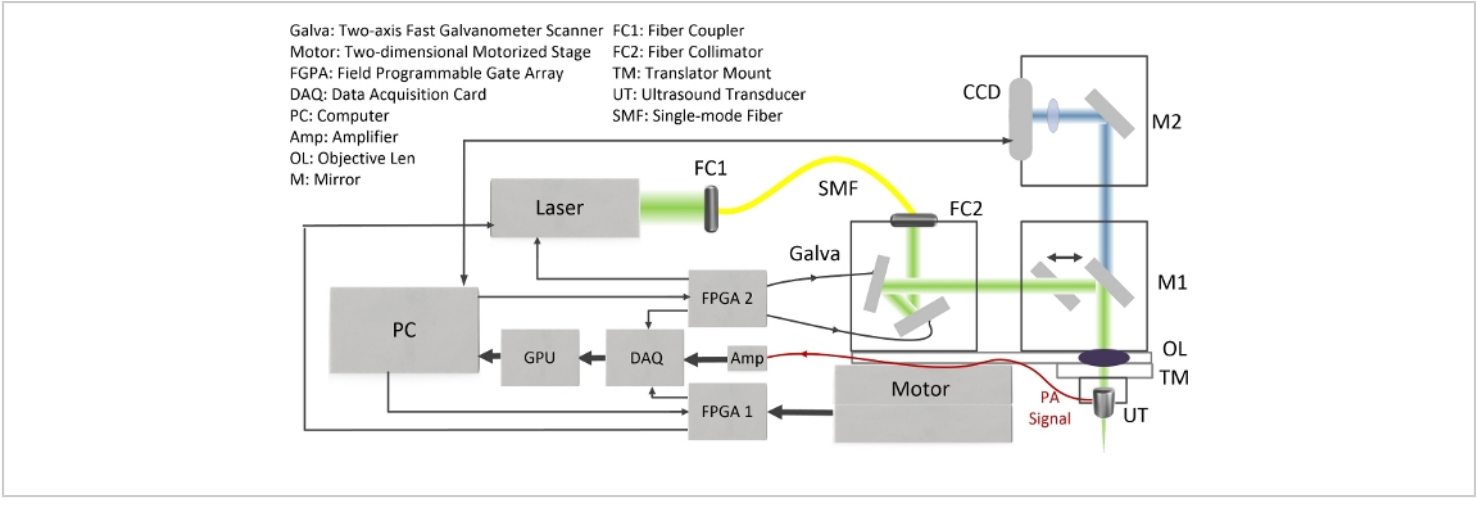

Figure 1: The schematic of DRS-PAI system. Please click here to view a larger version of this figure.

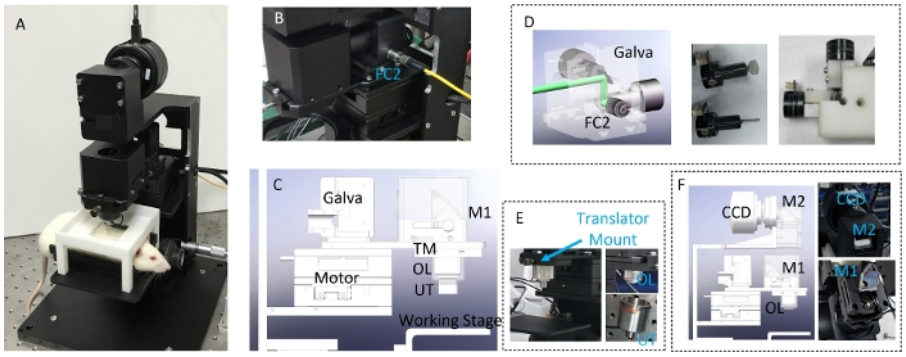

Figure 2: The design of DRS-PAI system.

(**A**) The photograph of DRS-PAI system. (**B**) The panel shows a photograph of the setup for laser path assembly. (**C**) The panel shows the 3D model for laser path assembly. (**D**) The panel shows the two-axis fast galvanometer scanner assembly. (**E**) The panel shows the probe assembly. (**F**) The panel shows the CCD optical path assembly. Please click here to view a larger version of this figure.

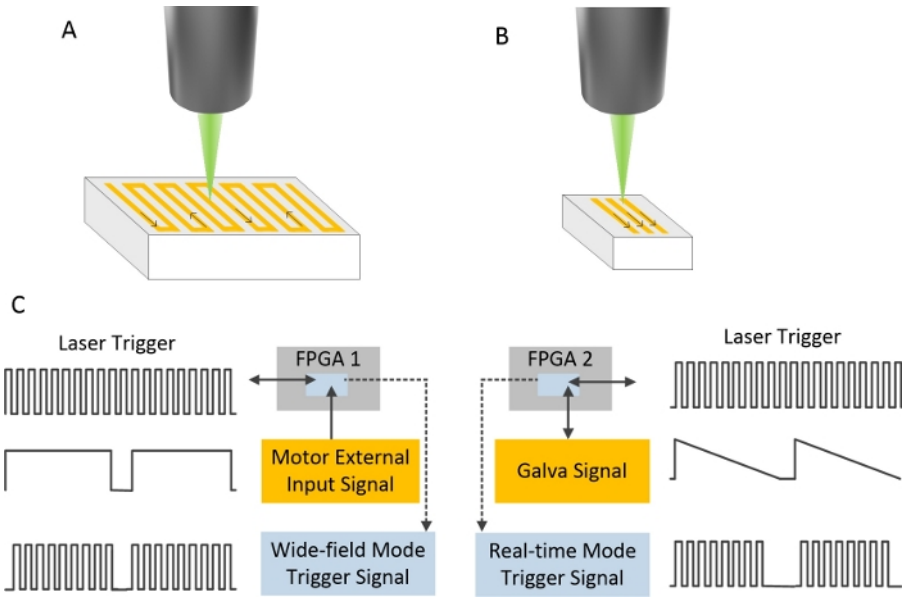

Figure 3: The setup of scan for different imaging modes.

(**A**) The scan path of WIM. (**B**) The scan path of RIM. (**C**) The trigger setup of two imaging modes. Please click here to view a larger version of this figure.

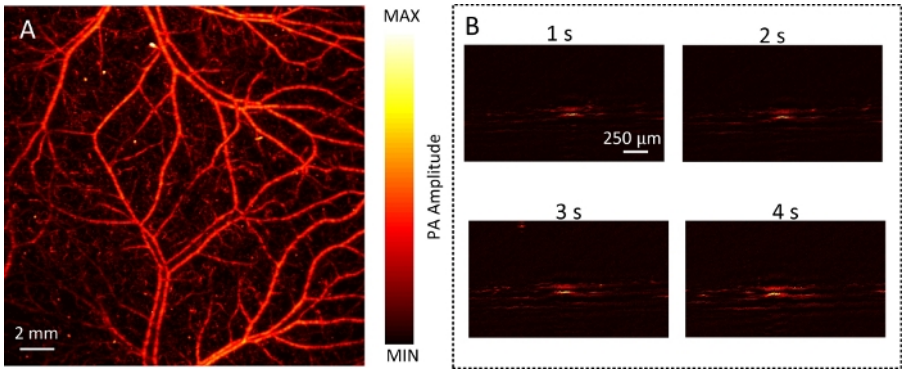

Figure 4: The photoacoustic WIM and RIM of the mouse back.

(**A**) The MAP image of mouse back in WIM. (**B**) The B-Scan images of mouse back in RIM. Please click here to view a larger version of this figure.

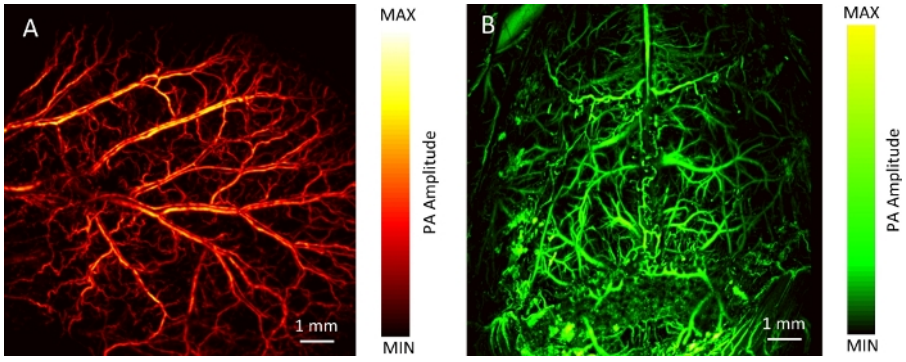

Figure 5: The photoacoustic WIM of a mouse.

(**A**) The MAP image of the mouse ear in WIM. (**B**) The MAP image of the mouse brain in WIM. Please click here to view a larger version of this figure.

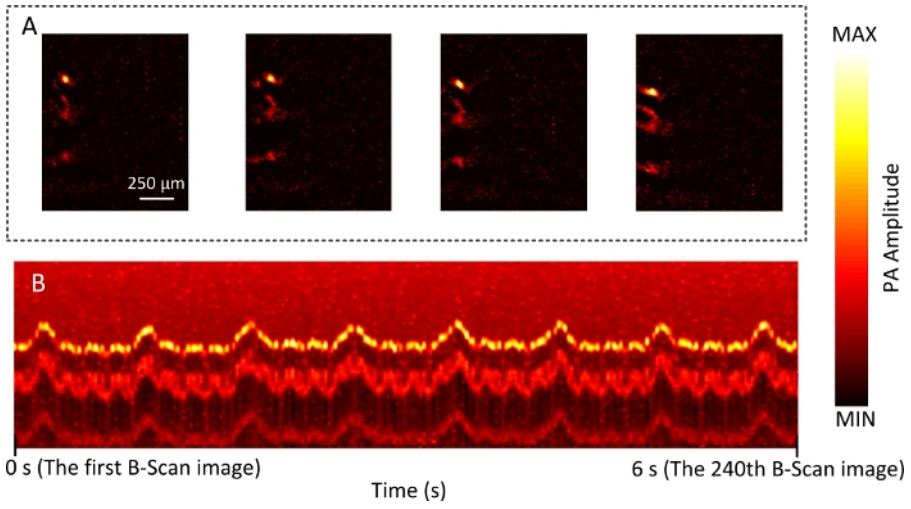

Figure 6: The photoacoustic RIM of the mouse abdomen.

(**A**) The B-scan images of the mouse abdomen in RIM. (**B**) The MAP image along the depth direction of the mouse abdomen versus time in RIM. Please click here to view a larger version of this figure.

Video 1: The process of RIM of the mouse back. Please click here to download this video.

Video 2: The process of MAP image along the depth direction of the mouse abdomen versus time. Please click here to download this video.

Supplementary Figure 1: The part of the imaging region in contact with the polyethylene membrane. Please click here to download this figure.

Discussion

Here we presented a dual raster-scanning photoacoustic small-animal imager for noninvasive vascular visualization which was designed and developed to capture the structure of the vasculature and the related dynamic change of blood. The advantage of DRS-PAI is that it integrates the WIM and the RIM into one system, which makes it easier to study vascular dynamic and vascular network structure of small animals. The system can provide high-resolution wide-field vascular visualization and real-time blood dynamics.

In the current system, the optical excitation was implemented with a single-wavelength light source. A future multi-wavelength system would provide other parameters such as blood oxygen saturation. Further, a special image processing algorithm can be developed for quantitative analysis, including estimating vascular diameter, vascular density, vascular tortuosity, etc. The quantitative analysis can provide valuable information for early diagnosis and treatment of diseases.

In summary, the system enables researchers to obtain high-dimensional physiological and pathological insights into small-animal research with biomedical relevance. The system can be adapted to most small-animal research settings, include but not limited to, imaging of angiogenesis, tumor microenvironments, hemodynamic, functional connections in

the brain, microcirculation, drug responses, and therapy responses. Critical steps within the protocol include the design of the dual scanning structure, the confocal adjustment of the optical and acoustic focus in the WIM, and center point adjustment of the sound field in the RIM.

Disclosures

All animal experiments were performed according to the approved guidelines and regulations of the Institutional Animal Care and Use Committee. The authors have no relevant financial interests in the manuscript and no other potential conflicts of interest to disclose.

Acknowledgments

The authors would like acknowledge the financial support from National Natural Science Foundation of China (61822505; 11774101; 61627827; 81630046), The Science and Technology Planning Project of Guangdong Province, China (2015B020233016), and The Science and Technology Program of Guangzhou (No. 2019020001).

References

1. Li, L., et al. Single-impulse panoramic photoacoustic computed tomography of small-animal whole-body dynamics at high spatiotemporal resolution. *Nature Biomedical Engineering.* **1**(5), 0071 (2017).
2. Jeon, S., Kim, J., Lee, D., Baik, J. W., Kim, C. Review on practical photoacoustic microscopy. *Photoacoustics.* **15**, 100141 (2019).
3. Baik, J. W., et al. Super wide-field photoacoustic microscopy of animal and humans *in vivo*. *IEEE Transactions on Medical Imaging.* **39** (4), 975-984 (2019).
4. Omar, M., Aguirre, J., Ntziachristos, V. Optoacoustic mesoscopy for biomedicine. *Nature Biomedical Engineering.* **3** (5), 354-370 (2019).
5. Lin, L., et al. Single-breath-hold photoacoustic computed tomography of the breast. *Nature Communications.* **9** (1), 2352 (2018).
6. Yang, F., et al. Wide-field monitoring and real-time local recoding microvascular networks on small animals with a dual-raster-scanned photoacoustic microscope. *Journal of Biophotonics.* **13** (6), e202000022 (2020).
7. Sun, J., Zhou, Q., Yang, S. Label-free photoacoustic imaging guided sclerotherapy for vascular malformations: a feasibility study. *Optics Express.* **26** (4), 4967-4978 (2018).
8. Xu, D., Yang, S., Wang, Y., Gu, Y., Xing, D. Noninvasive and high-resolving photoacoustic dermoscopy of human skin. *Biomedical Optics Express.* **7** (6), 2095-2102 (2016).
9. Zhang, W., et al. Miniaturized photoacoustic probe for *in vivo* imaging of subcutaneous microvessels within human skin. *Quantitative Imaging in Medicine and Surgery.* **9** (5), 807-814 (2019).
10. Chen, Q., et al. Ultracompact high-resolution photoacoustic microscopy. *Optics Letters.* **43** (7), 1615-1618 (2018).
11. Lan, B., et al. High-speed widefield photoacoustic microscopy of small-animal hemodynamics. *Biomedical Optics Express.* **9**, 4689-4700 (2018).
12. Ma, H., Yang, S., Cheng, Z., Xing, D. Photoacoustic confocal dermoscope with a waterless coupling and impedance matching opto-sono probe. *Optics Letters.* **42** (12), 2342-2345 (2017).

13. Kang, H., Lee, S. W., Lee, E. S., Kim, S. H., Lee. T. G. Real-time GPU-accelerated processing and volumetric display for wide-field laser-scanning optical-resolution photoacoustic microscopy. *Biomedical Optics Express.* **6** (12), 4650-4660 (2015).